$Co_{1-x}Fe_xS_2$: A Tunable Source of Highly Spin-Polarized Electrons

L. Wang,[1] K. Umemoto,[1,2] R. M. Wentzcovitch,[1,2] T. Y. Chen,[3] C. L. Chien,[3] J. G. Checkelsky,[4] J. C. Eckert,[4] E. D. Dahlberg,[5] and C. Leighton[1]

[1]*Department of Chemical Engineering and Materials Science, University of Minnesota, USA*
[2]*Minnesota Supercomputer Institute for Digital Technology and Advanced Computation, University of Minnesota, USA*
[3]*Department of Physics and Astronomy, Johns Hopkins University, USA*
[4]*Physics Department, Harvey Mudd College, USA*
[5]*School of Physics and Astronomy, University of Minnesota, USA*

(Received 4 October 2004; published 11 February 2005)

In the emerging field of spin-electronics ideal ferromagnetic electron sources would not only possess a high degree of spin polarization, but would also offer control over the magnitude of this polarization. We demonstrate here that a simple scheme can be utilized to control both the magnitude and the sign of the spin polarization of ferromagnetic CoS_2, which we probe with a variety of techniques. The position of the Fermi level is fine-tuned by solid solution alloying with the isostructural diamagnetic semiconductor FeS_2, leading to tunable spin polarization of up to 85%.

DOI: 10.1103/PhysRevLett.94.056602 PACS numbers: 72.25.Ba, 75.47.–m, 85.75.–d

The goal of ''spin electronics'' is to utilize the electron's spin, in addition to its charge, to create new electronic devices or enhance the functionality of current ones [1]. A fundamental component in any such device is a ferromagnetic (F) electrode which is used as a source of polarized electrons. For many devices high values of the F spin polarization at the Fermi level, P, provide significant benefits, e.g., large tunneling magnetoresistance (MR) [2–5] and ''Ohmic'' spin injection [6] into semiconductors [7]. This situation has stimulated extensive efforts to find materials, the so-called half-metallic ferromagnets (HMFs), with $P = 100\%$ [1,8]. This research has generally involved surveying potential HMFs by theoretical band-structure calculations, identifying promising candidates, and then measuring P in experimental investigations. Although difficulties exist with these measurements, notable successes have been achieved including establishment of $P \approx 100\%$ by several methods in CrO_2 [9–12], $P = 100\%$ at low T in $La_{1-x}Sr_xMnO_3$ [13,14], and P up to 80% in Fe_3O_4 [4,15,16].

Ideally, fundamental studies require materials that, in addition to being highly polarized, have *tunable* P, allowing for characterization of device parameters (e.g., tunneling MR, injection efficiency) as a function of the polarization of the electrodes. We demonstrate here a simple scheme to fabricate a tunable source of spin-polarized electrons that avoids the labor-intensive surveying of candidate compounds, moving instead towards a situation where a HMF can be *engineered* by Fermi level control. Our work is based on the pyrite structure (Fig. 2, inset) itinerant ferromagnet CoS_2 ($T_C = 121$ K, electronic configuration $t_{2g}^6 e_g^1$, $S = 1/2$) [17]. Our recent determination of $P = 56\%$ from point contact Andréev reflection (PCAR) confirms that the pure compound is *not* half metallic [18]. The essential concept, which was alluded to by Zhao *et al.* [19] and put on a firm theoretical footing by Mazin [20], is illustrated in Fig. 1(a) and exploits the fact that CoS_2 has a Fermi level (E_F) that lies low in the conduction band and that it can be alloyed with FeS_2, an isostructural diamagnetic semiconductor ($t_{2g}^6 e_g^0$, $S = 0$) [19–22], with a decreased E_F. The solid solution $Co_{1-x}Fe_xS_2$ is then expected to have an x dependent Fermi level, implying that in a certain composition range E_F can be decreased such that it intersects the majority spin band while lying in a gap for the minority spins, producing $P = 100\%$ [see Fig. 1(a)].

In order to verify the essential features of this picture, we performed electronic structure calculations, as summarized in Fig. 1(b) for $x = 0.00$, 0.125, and 0.25. The calculations employed the local-spin-density approximation (LSDA) [23] for the electronic exchange-correlation interaction, with Vanderbilt [24], Rappe-Rabe-Kaxiras-Joannopoulos [25], and Bachelet-Hamann-Schlüter [26] pseudopotentials for Co, Fe, and S, respectively. Calculations were performed with the PWSCF package [27]. We used 119 k points in the irreducible wedge of the Brillouin zone of the primitive cell and a plane-wave cutoff energy of 30 Ry. $Co_{1-x}Fe_xS_2$ solid solutions were described by an ordered supercell approach (e.g., Co_7FeS_{16} for $x = 0.125$, etc.) using equivalent sets of k points. The effect of disorder (i.e., random alloy versus ordered supercell) on the density of states (DOS) and the saturation magnetization were addressed by Mazin [20] and found to be small. We used the same (experimental) crystal structure parameters for all alloy compositions ($a = 5.524$ Å and $u = 0.389$ for $0 < x < 0.3$ in $Co_{1-x}Fe_xS_2$) [28]. A detailed discussion of the band structure and DOS, including more calculational details and a comparison between the various theoretical methods will be provided elsewhere [29]. Our electronic band structure is indistinguishable from that obtained by Shishidou *et al.* [30] using the full-potential linear augmented-plane-wave method in conjunction with the LSDA. However, our DOS obtained using the linear tetrahedral method of summation differs in small but important details from Shishidou's in the vicinity of E_F. In contrast to

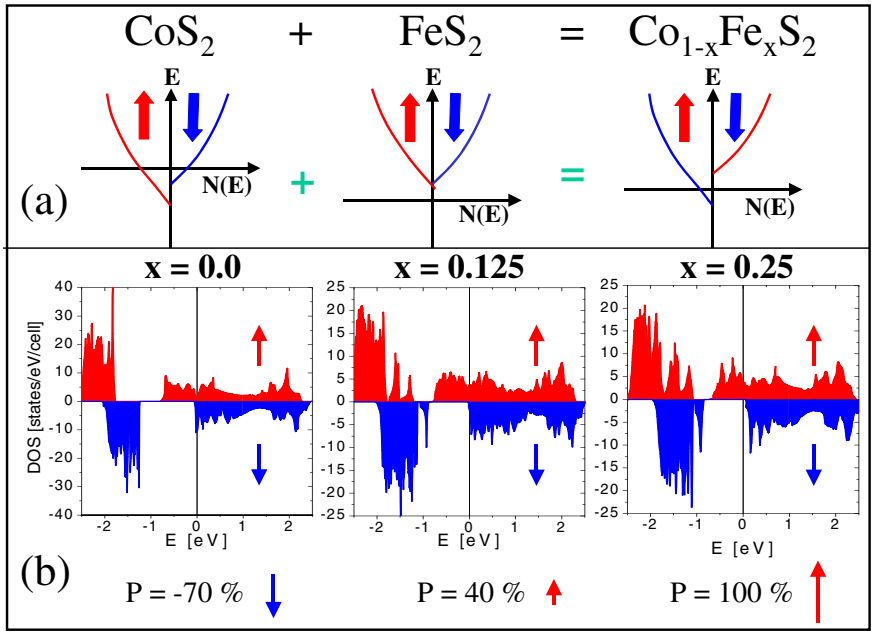

FIG. 1 (color online). (a) Schematic depiction of the basic concept of composition control of E_F and P in $Co_{1-x}Fe_xS_2$. (b) Calculated DOS for $x = 0.00$, 0.125, and 0.25. The value of P in each case is shown underneath the figure. E_F is taken as the zero point of energy.

that calculation, and quite interestingly, we find that CoS_2 is actually a minority spin system, due to the sharp feature in the minority DOS at E_F. Increasing Fe doping leads to the anticipated decrease in E_F and a situation at $x = 0.125$ where E_F just bisects the minority spin band but has a large majority DOS. Fe doping therefore induces an unexpected sign change in P. Further doping decreases E_F into the gap for the minority spins while maintaining a large DOS at E_F for the majority spins, yielding $P = 100\%$ at $x = 0.25$, i.e., half-metallic ferromagnetism.

Encouraged by these results, we fabricated bulk polycrystalline $Co_{1-x}Fe_xS_2$ paying special attention to the stoichiometry. Consistent with previous literature [31] we were unable to synthesize substitutional solid solutions by conventional solid-state reaction. Instead, we developed a new synthesis route based on reaction in the liquid phase, in an excess S vapor, followed by resulfurization at relatively low T. CoS_2 and FeS_2 powders (250 mg in total) were thoroughly ground and sealed in a quartz tube with 800 mg of S powder, which was subsequently evacuated to $<1 \times 10^{-6}$ Torr. The powder was then heated to 1100 °C (just above the melting point of both constituents) to encourage a homogeneous substitutional solution. To counter the small amount of phase separation that occurs on cooling, the reaction product was reground and heated again in 150 mg S for 7 days at 900 °C, i.e., just below the melting point. The resulting powder was found to be a homogeneous substitutional solid solution (see below for structural characterization) but with significant S deficiency due to the high temperature processing, which favors thermal dissociation of CoS_2. In order to achieve the desired stoichiometry, and to produce a dense sintered pellet for transport measurements, the powders were then cold pressed under 9×10^5 psi and resulfurized at 700 °C with 150 mg of S. Scanning electron microscopy reveals an average grain size of 10 μm. The x-ray diffraction (Fig. 2, inset) can be indexed to the pyrite structure with no evidence of any impurity phases. The lattice parameter deduced from the (200) peak shows the expected shift with x (Fig. 2), following Vegard's law, and demonstrating a substitutional solid solution. Significantly, the (200) peak width is largely independent of x. Energy dispersive spectroscopy indicates a composition of $(Co, Fe)S_{2.2}$, i.e., excess S. A previous attempt to engineer high P in $Co_{1-x}Fe_xS_2$ single crystals resulted in disappointing P values (47%–61%) and a weak dependence on x [32], which was attributed to a measured S deficiency up to 10%. Clearly in our case this S deficiency problem is alleviated, likely due to the enhanced grain boundary S diffusion rate in polycrystals [33], compared to single crystal specimens.

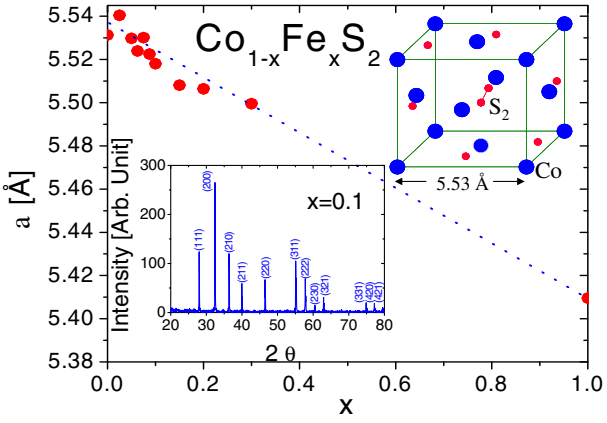

FIG. 2 (color online). x dependence of the experimental lattice parameter. Solid points are data, while the blue or dark grey dotted line is Vegard's law. Lower inset: X-ray powder diffraction from a representative sample ($x = 0.10$). Upper inset: Crystal structure of $Co_{1-x}Fe_xS_2$. Blue or dark grey circles are the Co(Fe) atoms; red or light grey circles represent the S atoms.

Following the fabrication of the stoichiometric polycrystals, we made a number of measurements to probe P, including (i) the low T saturation magnetization (M_S), (ii) the high field (90 kOe) MR at $T < T_C$, (iii) the low T anisotropic magnetoresistance (AMR), and (iv) PCAR. M_S is a simple indicator of P, as it is well known [1,8] that $P = 100\%$ implies an integer number of μ_B/Co ion (1.0 in this case). The essential idea behind the use of high field MR as a probe of P is that in a conventional ($P < 100\%$) F at $0\ \mathrm{K} < T < T_C$ negative MR occurs due to field-induced suppression of spin-flip electron-magnon scattering [18]. In a HMF, however, the absence of minority states eliminates the possibility of spin-flip scattering events leading to a vanishing of this MR. This has been observed in CrO_2 at ≈ 80 K, coincident with the disappearance of spin-flip scattering in the T dependence of the resistivity, ρ [34]. According to the basic theoretical formulations, the AMR in F metals can also be used as a probe of spin polarization, as it is sensitive to the *sign* of P. Specifically, McGuire and Potter [35] predict that a minority spin F is expected to have a negative AMR (i.e., ρ with the field perpendicular to the current is larger than with the field parallel), and vice versa. PCAR was used as the final, and most direct, probe of P [36] and was performed with both Pb and NbN tips. P was estimated by measurement of multiple contacts followed by extrapolation to $Z = 0$ [14], where Z is the dimensionless quantity used to describe the strength of the interfacial barrier [37]. Note that the insensitivity of PCAR to the sign of P means that it is particularly important that we employ AMR as an independent probe of the sign.

Figure 3 shows the results of the application of these various techniques as a function of Fe doping. As previously discussed, the theoretical P first reverses sign and then reaches 100% at $x = 0.25$. The corresponding theoretical M_S [Fig. 3(b)] takes a noninteger value at $x = 0.00$ (consistent with $P < 100\%$), which increases with x reaching exactly 1.0 μ_B/Co at $x = 0.25$. The experimental results of Fig. 3(c) reveal good agreement with the theoretical prediction in Fig. 3(b). An M_S of 1.0 μ_B/Co is achieved at $x \approx 0.07$ and is maintained up to $x = 0.30$. These data are therefore consistent with the attainment of a HMF state at $x = 0.07$, although they do not constitute direct proof. Further evidence is provided by the high field MR [Fig. 3(d)] which was measured at $T = 0.5T_C$ at each x value. Consistent with $P < 100\%$, significant negative MR is observed at $x = 0.00$ due to the expected field-induced suppression of spin-flip scattering. In agreement with the $M_S(x)$ data (which attains 1.0 μ_B/Co at $x = 0.07$) this negative MR vanishes at exactly $x = 0.07$, where it is replaced with a small positive contribution that peaks at T_C. The remarkable agreement between the x value for the attainment of $M_S = 1.0$ μ_B/Co and the vanishing of the high field MR must be considered as strong evidence for a highly polarized state at $x \geq 0.07$. The x dependence of the AMR [Fig. 3(e)] is also consistent with this scenario. The AMR is negative for undoped CoS_2 but reverses sign at $x \sim 0.03$, which we interpret [35] as a crossover from minority spin to majority spin behavior, as predicted by our calculations. Note that the vertical dotted lines in Fig. 3 indicate the positions of the sign reversal in P and the apparent attainment of $P = 100\%$. Discrepancies exist between experiment and theory on the positions of these special Fe doping levels, a point which will be returned to later.

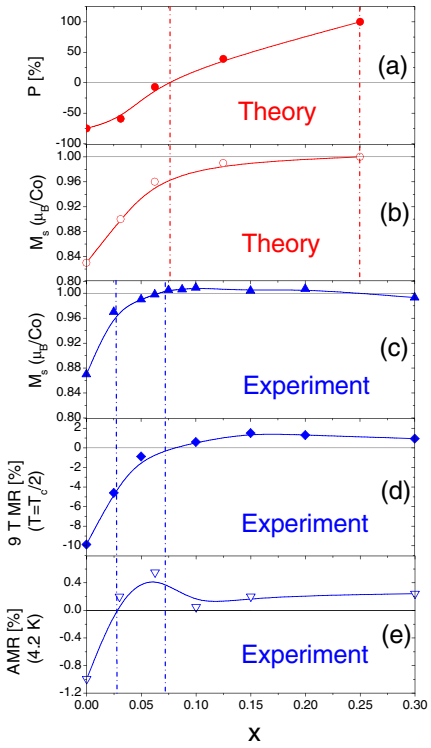

FIG. 3 (color online). x dependence of (a) the theoretical P, (b) the theoretical M_S, (c) the experimental M_S (assuming no moment on Fe), (d) the high field (9 T) MR at $\approx 0.5T_C$, and (e) the experimental AMR at 4.2 K. AMR is defined as $(\rho_{\|} - \rho_{\perp})/\rho(0)$, where $\rho_{\|}$ is the resistivity measured with field parallel to current, $\rho_{\perp}$ is the resistivity measured with field perpendicular, and $\rho(0)$ is the zero field value.

The PCAR of Fig. 4 provides a more direct probe of P. The main panel shows the normalized conductance versus voltage normalized to the superconducting gap, for $x = 0.00$, 0.08, 0.15, and 0.30. The data correspond to the smallest measured Z value (which is provided in the legend), and the solid lines are best fits to the model of Strijkers *et al.* [38]. Even without fitting it is clear from the extent of the subgap conductance suppression that P increases rapidly with x, reaching as much as 85% at $x = 0.15$. The typical [10,38] decrease in $P(Z)$ is observed, and it is the $Z = 0$ extrapolations that are shown as a function of x in the inset. For direct comparison the inset also shows the x dependence of the *magnitude* of the theoretical P [from Fig. 3(a)]. (The magnitude is plotted because, as previously mentioned, PCAR is insensitive to the sign of P.) Once again the agreement is noteworthy. The band-structure calculations predict an initial decrease followed by a sharp increase at $x = 0.07$ due to the sign reversal. Although experimental data provide only weak evidence of

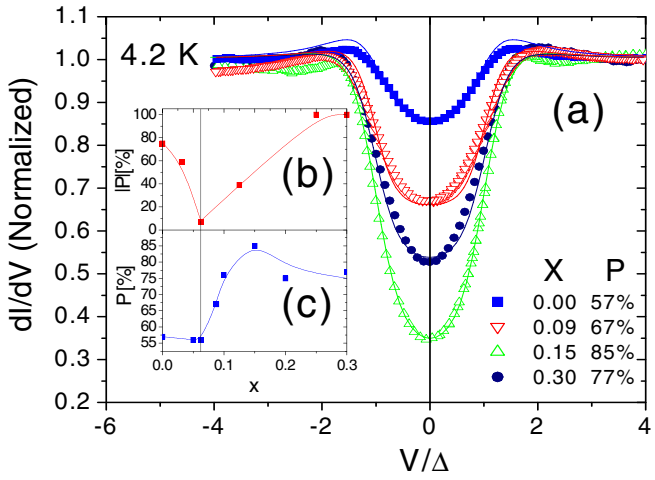

FIG. 4 (color online). (a) 4.2 K conductance (normalized to the normal state), as a function of voltage (normalized to the superconducting gap), for $x = 0.00$, 0.08, 0.15, and 0.30. Points represent experimental data, while the solid lines are fits as described in the text. Fitting parameters are $x = 0.00$, $P = 57\%$, $Z = 0.00$; $x = 0.08$, $P = 56\%$, $Z = 0.09$; $x = 0.15$, $P = 80\%$, $Z = 0.28$; and $x = 0.30$, $P = 73\%$, $Z = 0.09$. Inset: x dependence of (b) the *magnitude* of the theoretical P, and (c) the experimentally determined P.

this initial decrease, it is clear that P increases sharply around $x = 0.07$, eventually reaching 85% at $x = 0.15$.

Despite the encouraging PCAR and the consistency of the other methods for indirectly probing P, discrepancies remain between theory and experiment. The absence of the initial decrease in the experimental $P(x)$, the saturation of P at $<100\%$, and the disagreement with theory on the Fe doping levels for a reversal in spin polarization and onset of an apparent half-metallic state are problematic. There are a number of possible sources of discrepancy. First, the definition of P in terms of $N(E_F)$, as employed in our calculations, is not directly comparable to PCAR, which actually measures the polarization of a current [39]. This spin-polarized current is weighted by the (spin-dependent) Fermi velocity, or its square, depending on whether the contact is in the ballistic or diffusive regime [39]. It is likely that this is the source of the discrepancy at low x where the sign change occurs according to calculations. Second, the samples used appear to have a random Fe distribution, while the calculations require the use of supercells, which model ordered alloys. The work of Mazin [20], however, suggests that this may not in fact present a significant source of error. Finally, it is possible that small discrepancies could arise due to surface effects which are neglected in the calculations.

In summary, we have demonstrated the feasibility of a simple scheme for engineering high spin polarization in $Co_{1-x}Fe_xS_2$ by alloy control of the Fermi level. A combination of indirect transport probes, direct measurement by PCAR, and electronic structure calculations provides a consistent picture where the spin polarization can be continuously tuned in the range $-56\% < P < +85\%$. Along with the close lattice match to technologically relevant materials such as Si and GaAs, this opens up the possibility of employing these materials as tunable sources of polarized electrons for fundamental studies in spin electronics.

Work at UMN was supported primarily by the MRSEC Program of the NSF under DMR-0212302. R. M. W. acknowledges financial support from NSF DMR-0325218. Work at JHU was supported by NSF DMR-0080031.

[1] S. A. Wolf *et al.*, Science **294**, 1488 (2001).
[2] M. Bowen *et al.*, Appl. Phys. Lett. **82**, 233 (2003).
[3] G. Hu and Y. Suzuki, Phys. Rev. Lett. **89**, 276601 (2002).
[4] J. S. Parker *et al.*, Phys. Rev. B **69**, 220413(R) (2004).
[5] A. Gupta and J. Z. Sun, J. Magn. Magn. Mater. **200**, 24 (1999).
[6] R. Fiederling *et al.*, Nature (London) **402**, 787 (1999); Y. Ohno *et al.*, Nature (London) **402**, 790 (1999).
[7] G. Schmidt *et al.*, Phys. Rev. B **62**, R4790 (2000).
[8] C. M. Fang *et al.*, J. Appl. Phys. **91**, 8340 (2002).
[9] K. P. Kamper *et al.*, Phys. Rev. Lett. **59**, 2788 (1987).
[10] Y. Ji *et al.*, Phys. Rev. Lett. **86**, 5585 (2001).
[11] E. J. Singley *et al.*, Phys. Rev. B **60**, 4126 (1999).
[12] J. S. Parker *et al.*, Phys. Rev. Lett. **88**, 196601 (2002).
[13] J.-H. Park *et al.*, Phys. Rev. Lett. **81**, 1953 (1998).
[14] B. Nadgorny *et al.*, Phys. Rev. B **63**, 184433 (2001).
[15] Y. S. Dedkov *et al.*, Phys. Rev. B **65**, 064417 (2002).
[16] S. A. Morton *et al.*, Surf. Sci. **513**, L451 (2002).
[17] H. Hiraka and Y. Endoh, J. Phys. Soc. Jpn. **63**, 4573 (1994).
[18] L. Wang *et al.*, Phys. Rev. B **69**, 094412 (2004).
[19] G. L. Zhao *et al.*, Phys. Rev. B **48**, 15 781 (1993).
[20] I. I. Mazin, Appl. Phys. Lett. **77**, 3000 (2000).
[21] S. K. Kwon *et al.*, Phys. Rev. B **62**, 357 (2000).
[22] H. S. Jarrett *et al.*, Phys. Rev. Lett. **21**, 617 (1968).
[23] P. Hohenberg and W. Kohn, Phys. Rev. **136**, B864 (1964); W. Kohn and L. J. Sham, Phys. Rev. **140**, A1133 (1965); J. P. Perdew and A. Zunger, Phys. Rev. B **23**, 5048 (1991).
[24] D. Vanderbilt, Phys. Rev. B **41**, R7892 (1990).
[25] A. M. Rappe *et al.*, Phys. Rev. B **41**, R1227 (1990).
[26] G. B. Bachelet *et al.*, Phys. Rev. B **26**, 4199 (1982).
[27] See http://www.pwscf.org.
[28] R. W. G. Wyckoff, *Crystal Structures* (Interscience, New York, 1965), Vol. 1.
[29] K. Umemoto *et al.* (unpublished).
[30] T. Shishidou *et al.*, Phys. Rev. B **64**, 180401 (2001).
[31] R. J. Bouchard, Mater. Res. Bull. **3**, 563 (1968).
[32] S. F. Cheng *et al.*, J. Appl. Phys. **93**, 6847 (2003).
[33] *Handbook of Grain and Interphase Boundary Diffusion*, edited by I. Kaur, W. Gust, and L. Lozma (Ziegler Press, Stuttgart, 1989).
[34] S. M. Watts *et al.*, Phys. Rev. B **61**, 9621 (2000).
[35] T. R. McGuire and R. I. Potter, IEEE Trans. Magn. **11**, 1018 (1975).
[36] R. J. Soulen *et al.*, Science **282**, 85 (1998); S. K. Upadhyay *et al.*, Phys. Rev. Lett. **81**, 3247 (1998).
[37] G. E. Blonder *et al.*, Phys. Rev. B **25**, 4515 (1982).
[38] G. J. Strijkers *et al.*, Phys. Rev. B **63**, 104510 (2001).
[39] I. I. Mazin, Phys. Rev. Lett. **83**, 1427 (1999).